Korean J. Chem. Eng., 39(7), 1872-1879 (2022)
DOI: 10.1007/s11814-021-1045-4

pISSN: 0256-1115
eISSN: 1975-7220

Efficient removal of Cr(VI) by spent coffee grounds: Molecular adsorption and reduction mechanism

Yue Hu, Meiting Zhi, Shilin Chen, Wenguan Lu, Yinlong Lai, and Xiaobing Wang†

School of Chemistry and Civil Engineering, Shaoguan University, Shaoguan, 512023, P. R. China
(*Received 14 October 2021 • Revised 28 November 2021 • Accepted 16 December 2021*)

Abstract−Spent coffee ground (SCG), a byproduct from the soluble coffee industry, is usually discarded as waste. The reutilization of SCG for the removal of toxic heavy metal ions is a novel research direction. Until recently, the molecular adsorption and reduction mechanism of Cr(VI) on SCG was barely investigated. In this study, SCG was used for the efficient removal of Cr(VI) at a concentration range of 2-100 mg/L, with a maximum Cr(VI) uptake up to 36.2 mg/g. Structural characterization and ATR-FTIR analysis indicated that SCG possessed abundant surface O and N- containing functional groups. The corresponding adsorption and reduction effects on the Cr(VI) removal were investigated by the carboxyl and hydroxyl groups elimination experiments and ATR-FTIR characterization, respectively. The results revealed that $HCrO_4^-$ ions were preliminarily adsorbed on SCG surfaced-COOH/-OH/-NH by the formation of hydrogen bond (SCG surfaced-COOH/-OH/-NH···$HCrO_4^-$), and quickly reduced to Cr(III) by the electron denoted by phenolic compounds, and then *in-situ* immobilized on the surface of SCG. The effect of Cr(VI) concentration, coexisting ions, and humic acid was systematically studied to optimize the removal of Cr(VI) wastewater. Column experiments provided a new substitution to restore the Cr(VI)-containing groundwater for the permeable reactive barrier application. Thus, the proposed study uncovered the intrinsic Cr(VI) removal mechanism at the molecular level and explored the application of SCG for the efficient removal of Cr(VI).

Keywords: Spent Coffee Ground, Cr(VI), Adsorption, Reduction

INTRODUCTION

Hexavalent chromium (Cr(VI)), primitively distributed in chromite ore, easily migrates into natural water due to ore extraction, leather tanning, and chromium plating [1-4]. Due to its fast mobility and high toxicity, Cr(VI) causes great harm to human health and aquatic organisms. Normally, the reduction of Cr(VI) to Cr(III) for lowering the toxicity and the stable immobilization of Cr(VI) was a major remediation strategy [5,6]. Even though various methods of adsorbent, reduction, ion exchange and biological enrichment have been reported, most of them are not cost-effective. Consequently, more economical and eco-friendly technologies for the removal of Cr(VI) are still urgently needed.

Spent coffee ground (SCG) is a residue from the soluble coffee industry, with an annual production of 6 billion kg per year reported by the International Coffee Organization [7]. Usually, SCG is disposed of as solid waste, or used as fertilizer, causing harm to the environment [8,9]. Therefore, research on the secondary use of SCG is being carried out in a variety of fields, such as value-added products, green energy production, and adsorbent [10-12]. Especially, SCG is used to remove heavy metal Cr(VI) due to its adsorption efficiency and antioxidants [13,14]. For example, Prabhakaran et al. compared the SCG and spent tea for Cr(VI) removal and found that the coffee ground exhibited 40 times faster Cr(VI) removal efficiency than that of spent tea, mainly attributed to the more reductive phenolic compounds of coffee ground [15]. Han et al. reported that the rate of Cr(VI) removal by SCG at freezing temperature increased 11 times compared to room temperature, mainly due to the enhanced local concentration of protons and phenolic compounds [16]. Besides the excellent Cr(VI) removal performance of SCG, the preliminary results barely investigated how the Cr(VI) ions were adsorbed and reduced by SCG at the molecular level. Normally, SCG contains lignocelluloses, residual caffeine and phenolic compound, thus endowing SCG with abundant surface functional groups [17,18]. Obviously, these surface functional groups, such as -COOH and -OH, would interact with Cr(VI) ions during the Cr(VI) removal process. However, the possible interaction between the functional groups and Cr(VI) and how these functional groups affect the adsorption and reduction of Cr(VI), is still unknown, which is vital for deeply understanding the intrinsic mechanism of Cr(VI) removal by SCG. Thus, it is of great significance for us to develop a promising approach for the utilization of SCG waste.

In this study, the adsorption and reduction of Cr(VI) on the surface of SCG were investigated for the first time. The structure and surface functional groups were systematically studied for uncovering the intrinsic Cr(VI) removal mechanism at a molecular level. In addition, Cr(VI) concentration, coexisting ions, humic acid and column experiments were systematically checked for further treatment of actual Cr(VI)-contaminated wastewater.

MATERIALS AND METHODS

1. Chemicals and Materials

Spent coffee grounds (SCG) were obtained from Kentucky Fried

†To whom correspondence should be addressed.
E-mail: 20180398@qq.com

Chicken (KFC), washed several times with distilled water, and dried at 60 °C in a vacuum oven. Analytical grade $K_2Cr_2O_7$, 1,10-phenanthroline, 1,5-diphenylcarbazide, NaCl, $NaNO_3$, Na_2SO_4, Na_2CO_3 and Na_3PO_4 were supplied by Sinopharm Chemical Reagent, China.

2. Characterization of Material

The structure of the SCG was studied by X-ray diffraction (XRD, Rigaku MiniFlex 600, Japan), scanning electron microscopy (SEM, HITACHI SU8010, Japan) combined with energy dispersive X-ray (EDX) imaging, and high-resolution X-ray photoelectron spectroscopy (XPS, VG Multilab 2000, USA). Surface functional groups of SCG were tested by ATR-FTIR spectroscopy (Nicolet iS50, Thermo Fisher Scientific, USA), at a resolution of 4 cm^{-1} and 100 scans. The specific surface area of SCG was measured by a Brunauer-Emmett-Teller method at 77 K (Micrometics ASAP2020, USA).

3. Cr(VI) Removal Procedure by SCG

Typically, a 0.1 g SCG sample was added to a 30 mL solution containing a certain concentration of Cr(VI) and shaken at 200 rpm at room temperature (25±2 °C). After a certain time interval, the supernatant was collected and analyzed using the 1,5-diphenylcarbazide colorimetric method (Fig. S1) [19]. For the regeneration, the Cr(VI)-adsorbed SCG was soaked in 30 mL of 0.1 mol/L nitric acid solution for 1 h and then washed several times with deionized water [20].

4. Removal of Cr(VI) by Carboxyl and Hydroxyl Groups on SCG

To evaluate the effect of carboxyl groups of SCG on the Cr(VI) removal, 0.5 g SCG was added to 18 mL anhydrous methanol and 2 mL HCl (37% wt). After being shaken continuously for 6 h, the sample was collected, washed with distilled water, and dried at 60 °C in a vacuum oven, and named "Eliminated-COOH of SCG". Similarly, for evaluating surface hydroxyl group on SCG, 0.5 g SCG was mixed with 20.0 mL HCHO solution, shaken for 6 h, and collected in the same way. The treated sample was named "Eliminated -OH of SCG".

5. Column Experiment

The inner diameter of the column reactor was 10 mm and the length was 160 mm. The bottom and top of the column were packed with 40 mm of quartz sand (10-20 mesh) and cotton to prevent the SCG loss from the column and to stabilize the SCG. 1 g SCG sample was filled into the middle of column. 2.0 mg/L of Cr(VI) was pumped through the column in an upflow mode at a flow rate of 0.5 mL/min. The empty bed contact time was 20 minutes. After a specific time, the effluent from the top of the column was collected for analysis.

RESULTS AND DISCUSSION

1. Cr(VI) Removal Efficiency of Spent Coffee Ground

The Cr(VI) removal efficiency of SCG was first investigated in a concentration range of 2-100 mg/L (Fig. 1(a)). The SCG showed a perfect removal performance at high Cr(VI) concentration. Specifically, at a concentration below 10 mg/L, SCG effectively removed 99.8% of Cr(VI) within one hour. With the increase of Cr(VI) concentration, the Cr(VI) removal rate slowly decreased. However, the total Cr(VI) removal capacity quickly increased from 2 to 30 mg/L (Table S1). The Cr(VI) removal capacity of SCG at different Cr(VI) concentrations was tested and described in Fig. 1(b). The Cr(VI) removal data were better fitted with the Langmuir model, consistent with Prabhakaran et al.'s report [15]. The maximum Cr(VI) removal capacity (q_m) of SCG reached 36.2 mg/g. After a specific

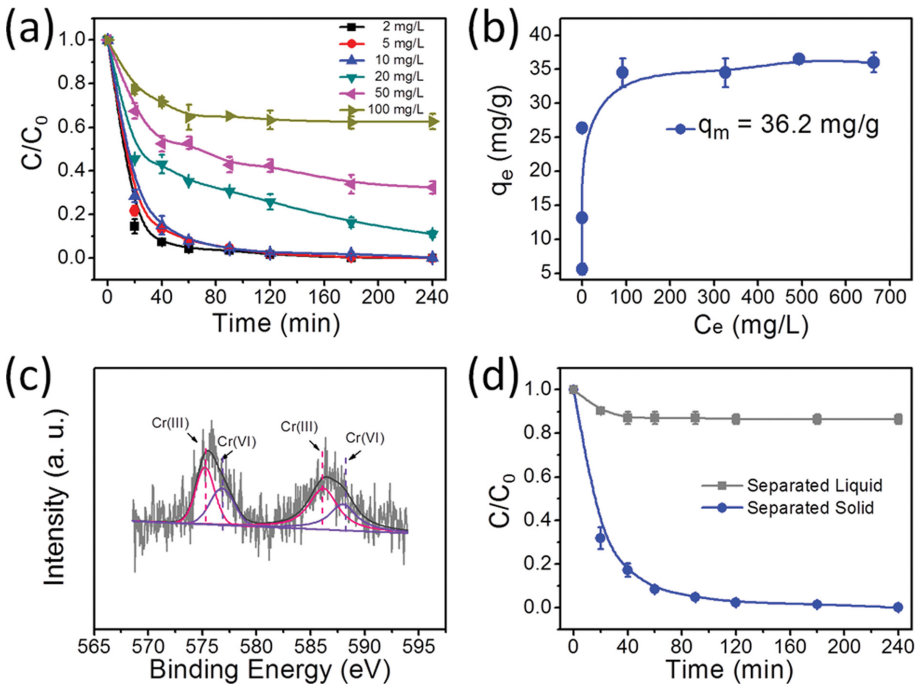

Fig. 1. (a) The removal efficiency of Cr(VI) by SCG under different Cr(VI) concentrations. (b) Adsorption isotherms of Cr(VI) on SCG. (c) Cr 2p HR-XPS spectroscopy of SCG reacted with Cr(VI). (d) Cr(VI) removal by the separated liquid and solid SCG. The dosage of SCG was 3.3 g/L. The initial pH was 6.5±0.1. For adsorption isotherms, the initial Cr(VI) concentration was 2 to 1,000 mg/L.

surface area was normalized, the maximum removal capacity was 7.40 mg/m^2 (Fig. S2). The value was higher than that of biochars [21,22], widely reported zero-valent iron-based adsorbents [23,24], and iron oxides [25,26], indicating its promising potential for the remediation of Cr(VI)-contaminated wastewater (Table S2). The outstanding Cr(VI) removal performance is mainly rooted in the special structure of SCG, which was explored in this study.

Subsequently, the reacted SCG was tested by HR-XPS spectroscopy. As shown in Fig. 1(c), an obvious Cr peak was observed, indicating that the reduced Cr(VI) in the solution was fixed on the SCG surface. By fitting the Cr 2p HR-XPS spectrum, the broad peak was attributed to Cr(III) and Cr(VI) species [27]. Especially, the Cr(III)/Cr(total) molar ratio reached 59%, further validating the promising reduction and immobilization capacity of SCG. Emphatically, to confirm the solid SCG itself for the Cr(VI) removal, we tested the Cr(VI) removal efficiency by the possible dissolved active substances from SCG. SCG was first added to 30 mL distilled water for a shocking 12 hours. Then, the separated liquid and SCG were separately applied to remove Cr(VI). Comparably, the separated liquid only removed 10% of Cr(VI), revealing the solid SCG was the

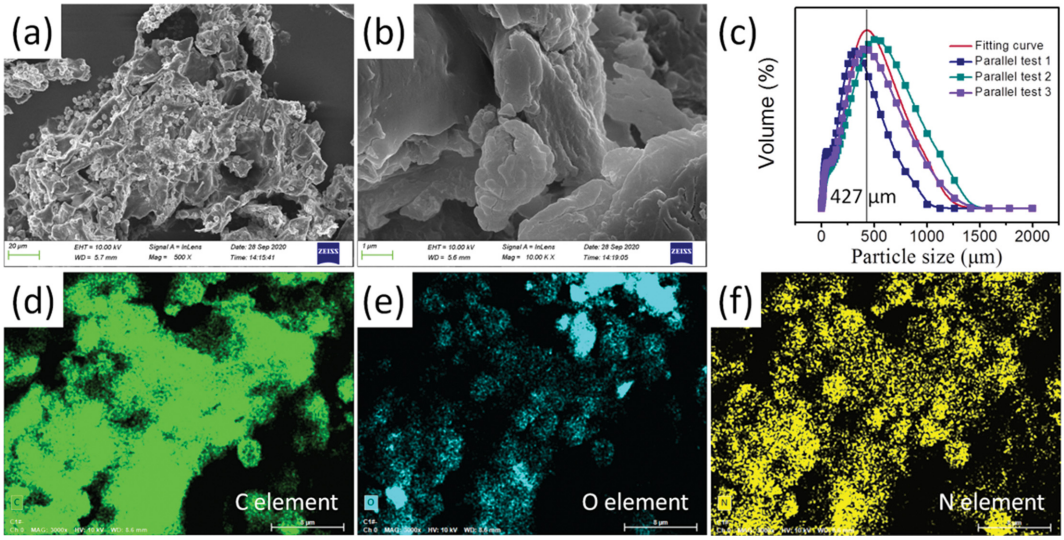

Fig. 2. (a), (b) SEM, (c) particle size, and (d)-(f) overlay of C, O, and N high-resolution EDS mapping of SCG.

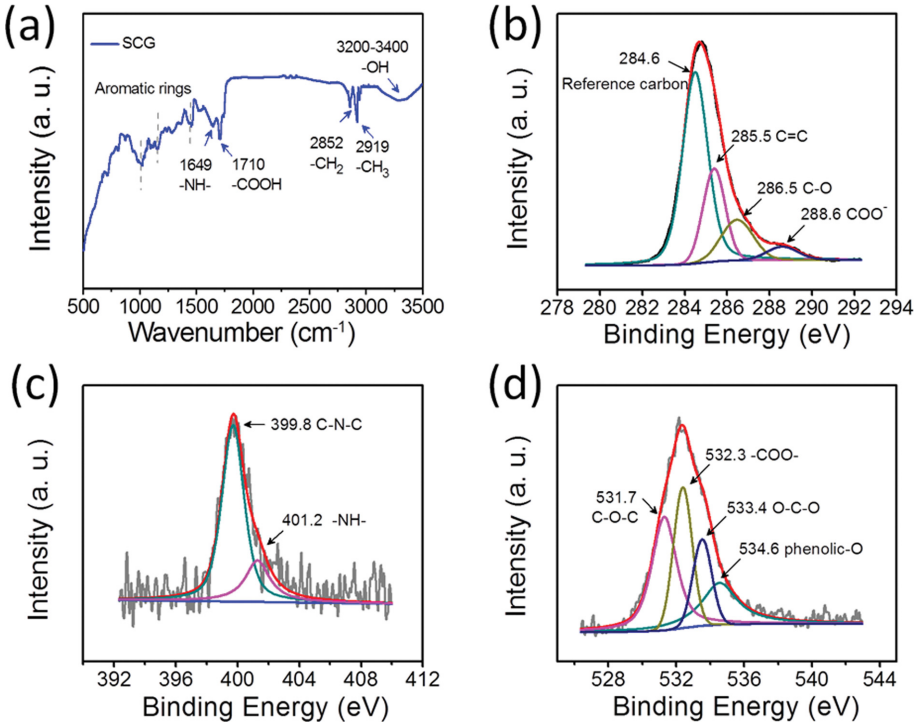

Fig. 3. (a) ATR-FTIR of SCG. Deconvoluted high-resolution XPS spectra of C 1s (b), N 1s (c), and O 1s (d).

main active substance to remove the Cr(VI) contaminant (Fig. 1(d)).

2. Structural Characterizations of SCG

To further clarify the Cr(VI) removal mechanism by the solid SCG, the SCG was subsequently characterized in detail. The morphology and surface element distribution of SCG was first examined and shown in Fig. 2. SEM images show that raw SCG exhibited an irregular block with a relatively smooth surface (Fig. 2(a), (b)). The average particle size of SCG was around 427 μm (Fig. 2(c)). EDS mapping analysis shows that the C, O, and N elements were evenly distributed on the surface of SCG, with the relative mass ratio of 73.7%, 18.8%, and 7.5%, respectively (Fig. 2(d)-(f) and Fig. S3).

ATR-FTIR was employed to analyze the surface functional groups on SCG. As shown in Fig. 3(a), a broad peak at 3,200-3,400 cm^{-1} indicates the O-H stretching and hydrogen bridges, mainly attributed to the phenolic hydroxyl and carboxyl groups [9,28]. Distinct peaks at 2,919 cm^{-1} and 2,852 cm^{-1} correspond to the symmetric stretching of $-CH_3$ and asymmetric stretching of $-CH_2-$, indicating the presence of lipid structure in SCG [29]. The bands at 1,710 cm^{-1} belong to the carboxyl bond vibrations from the various oxygen functional groups, while the bands at 1,649 cm^{-1} are attributed to the -NH- stretching of purine, indicating the presence of carbonyl compounds and caffeine [29,30]. The peaks at 1,460, 1,285, and 1,010 cm^{-1} are attributed to C=C bonds of aromatic rings, typical of lignins [20]. The above results confirm that SCG contains typical -OH, -COOH, and -NH- functional groups from lignocelluloses and other organic compounds. Additionally, the surface chemical environment of these functional groups was further checked by high-resolution XPS spectrum (Fig. S4). The presence of C, O, and N validated the results of SEM-EDS and ATR-FTIR. As shown in Fig. 3(b), the high-resolution C 1s XPS spectrum contains four peaks at 284.5, 285.4, 286.5, and 288.6 eV, respectively. A peak at 284.5 eV was designated as a reference carbon [23]. Another peak at 285.4 eV was ascribed to C=C bonds of the benzene ring, while the peak at 286.5 eV was attributed to C=O of the carboxyl group [20]. The low-intensity peak at 288.6 eV corresponds to the C-O of phenols [20]. Meanwhile, the N 1s spectrum analysis exhibits peaks assigned to C-N-C (purine N, 399.8 eV) and -NH- (401.2 eV), confirming the presence of caffeine (Fig. 3(c)) [31]. Additionally, the O peaks at 531.7 eV (C-O-C), 532.3 eV (-COO-), 533.4 eV (O-C-O), and 534.6 eV (phenolic-O) are ascribed to the carboxyl and phenolic hydroxyl groups (Fig. 3(d)) [7,32]. Thus, the ATR-FTIR analysis and high-resolution XPS spectra confirm that the SCG particles contain a mass of C-containing lignocelluloses, some N and O-containing organic compounds such as caffeine and phenolic compounds, endowing it with specific physicochemical properties for the removal of Cr(VI).

3. Effect of Surface Functional Groups on Cr(VI) Removal

ATR-FTIR spectrum was employed to study the surface functional group change of SCG after the removal of Cr(VI) (Fig. 4(a)). Obviously, the wide peak of -OH became weaker and the -COOH peak of reacted SCG nearly decreased, suggesting that the -OH and -COOH may be the main active sites to adsorb Cr(VI) [20]. Meanwhile, the peak intensity of -NH- at 1,649 cm^{-1} also weakened, meaning the interaction of the -NH- group with Cr(VI). How these O and N-containing functional groups attached with the Cr(VI) ions are important to unlock the mechanism of SCG for the Cr(VI) removal. Generally, Cr(VI) is absorbed on the absorbents via elec-

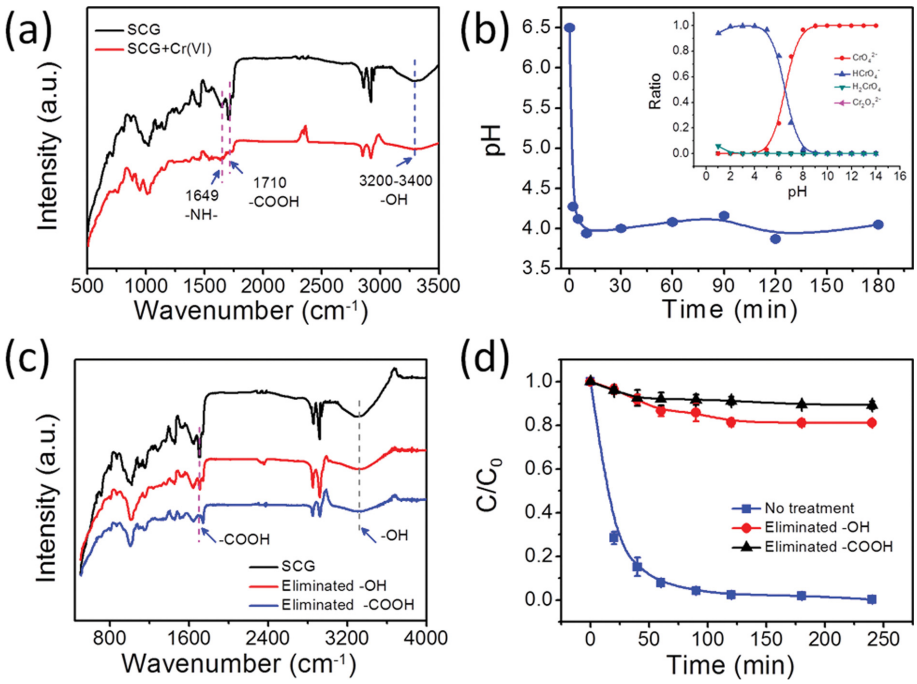

Fig. 4. (a) ATR-FTIR spectra of SCG reacting with Cr(VI). (b) pH change during the removal of Cr(VI) by SCG, and Cr(VI) speciation as a function of pH (Inset). (c) ATR-FTIR spectra of SCG, eliminated -OH and -COOH of SCG. (d) Cr(VI) removal efficiency by using SCG, eliminated -OH and -COOH of SCG. The dosage of SCG was 3.3 g/L. Initial pH and Cr(VI) concentration were 6.5±0.1 and 10 mg/L, respectively.

trostatic interaction, such as the electrostatic attraction between the positive and negative charged ions [33,34]. Therefore, the surface charge of SCG and Cr(VI) ions at different pHs were checked by zeta potential and Cr(VI) speciation simulation. The zeta potential of SCG at initial pH 4-8 was negative, which was mainly attributed to the existence of abundant negatively charged hydroxyl and carboxyl groups on SCG (Fig. S5). Meanwhile, the speciation of Cr(VI) ions as a function of pH was simulated (Inset in Fig. 4(b)). Therein, the main speciation below pH 4.5 was $HCrO_4^-$, above pH 9.0 was $Cr_2O_7^{2-}$, and between pH 4.5-9.0 was the co-existence of CrO_4^{2-} and $HCrO_4^-$. Additionally, the pH change during the Cr(VI) removal process was tested (Fig. 4(b)). The pH quickly decreased from 6.5 to 3.7 within 5 minutes and then slightly increased to 4.0 in 180 minutes, in which the SCG was negatively charged and Cr(VI) existed as $HCrO_4^-$ in the main speciation. Accordingly, the $HCrO_4^-$ anions could not be adsorbed on the negatively charged surface of SCG via electrostatic interaction [35]. Based on the above ATR-FTIR spectra analysis, we speculated that the $HCrO_4^-$ anions were adsorbed on the surface of SCG, mainly driven by the hydrogen bond formed between the O and N-containing functional groups on SCG and $HCrO_4^-$ anions [36]. During the adsorption process of $HCrO_4^-$, the hydrogen atoms of hydroxyl/carboxyl and -NH- groups are easily bonded with the highly electronegative O atom from the $HCrO_4^-$ anions to generate the hydrogen bond of -COOH/-OH···$HCrO_4^-$ and -NH···$HCrO_4^-$ (Eq. (1)-(3)), leading to the peak intensity decline of the corresponding -OH, -COOH and -NH- functional groups over SCG. Subsequently, the -COOH and -NH-containing compounds, like purine and lignin with the weaker reducibility, only adsorbed the $HCrO_4^-$ anions through the formed hydrogen bond [7,15]. In comparison, the phenolic compound with strong reducibility could transfer its electron to the absorbed $HCrO_4^-$ anions through the linked hydrogen bond and the reductive Cr(III) was *in-situ* immobilized on SCG [37], in which the molar ratio of Cr(III)/Cr(total) accounted for 59% revealed by the result of Cr 2p HR-XPS (Eq. (4)).

$$SCG\text{-}OH+HCrO_4^- \rightarrow SCG\text{-}OH\cdots HCrO_4^- \quad (1)$$

$$SCG\text{-}COOH+HCrO_4^- \rightarrow SCG\text{-}COOH\cdots HCrO_4^- \quad (2)$$

$$SCG\text{-}NH\text{-}+HCrO_4^- \rightarrow SCG\text{-}NH\cdots HCrO_4^- \quad (3)$$

$$HCrO_4^- + 7H^+ + 3e^- \rightarrow Cr^{3+} + 4H_2O \quad (4)$$

4. Main Roles of Surface -OH and -COOH Groups

To further confirm the key roles of surface -OH and -COOH groups of SCG on the Cr(VI) removal, the ATR-FTIR spectra and the Cr(VI) removal performance with the eliminated O-containing functional groups of SCG were checked. As was reported, the -OH groups could be eliminated by the reaction with formaldehyde, while the -COOH groups were blocked by shaking in anhydrous methanol and 0.1 mol/L HCl according to the reaction, Eq. (5) and Eq. (6) [20]. As shown in Fig. 4(c) of ATR-FTIR spectra, the corresponding peak intensity of -OH decreased for the eliminated -OH of SCG, while a blue shift of the -COOH peak occurred for the eliminated -COOH of SCG due to the formation of ester (Eq.

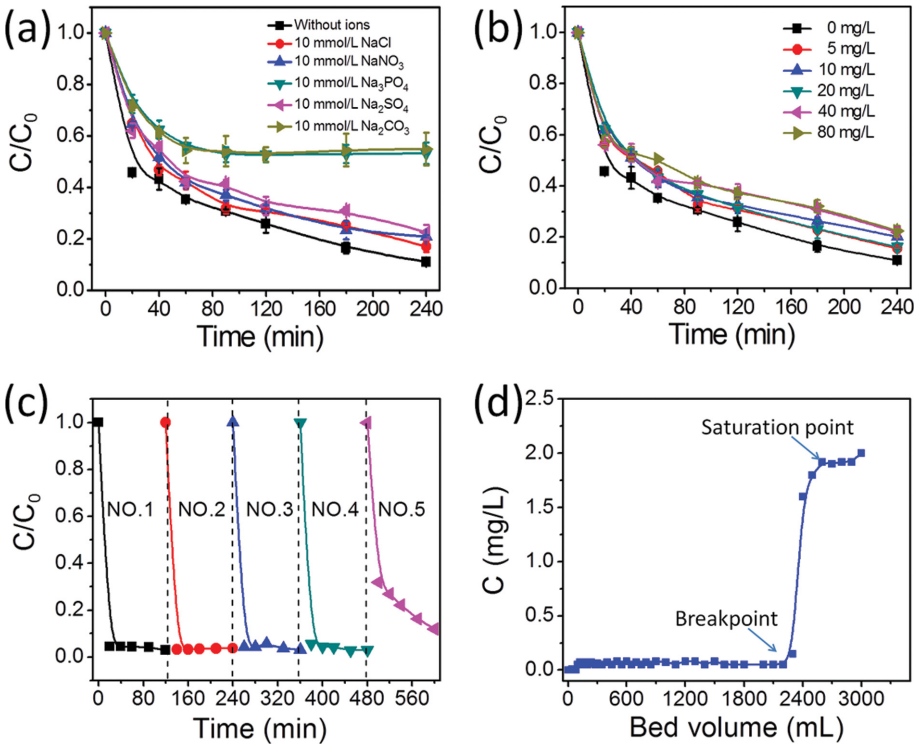

Fig. 5. (a), (b) Effect of co-existing ions and humic acid on the Cr(VI) removal by SCG. The initial concentration of SCG and Cr(VI) was 3.3 g/L and 20 mg/L, respectively. (c) Reusable performance of SCG in the consecutive removal of Cr(VI). The initial concentration of SCG and Cr(VI) was 3.3 g/L and 5 mg/L, respectively. (d) A typical breakthrough curve for SCG showing the movement of the mass transfer zone (influent Cr(VI) was 2.0 mg/L, influent pH was 6.5±0.1, the influent rate was 0.5 mL/min).

(6)). The Cr(VI) removal experiments revealed that the Cr(VI) removal efficiency with the eliminated -OH and -COOH of SCG was only 20.0%, 10.0%, respectively, much lower than the 99.9% with SCG (Fig. 4(d)). It could be interpreted that when the -COOH group was shielded by the formation of ester, the adsorption process of Cr(VI) by -COOH group of SCG was inhibited, and thus only -OH and -NH- groups with weak adsorption ability were responsible for the low efficiency for 20% of Cr(VI) removal. As for the elimination of -OH group, only 10% of Cr(VI) could be removed by the -COOH groups on SCG, although -COOH groups possessed a strong adsorption ability. This phenomenon well confirms the considerable synergistic effect of reduction promoting adsorption, which was consistent with Li et al. and Wang et al's reports [38,39]. These crucial findings highlight the important roles of the O- and N-containing groups on the adsorption and reduction of Cr(VI) at the molecular level.

$$2\text{SCG-OH}+\text{HCHO}\rightarrow(\text{SCG-O})_2\text{CH}_2+\text{H}_2\text{O} \quad (5)$$

$$\text{SCG-COOH}+\text{CH}_3\text{OH (acidic)}\rightarrow\text{COOCH}_3+\text{H}_2\text{O} \quad (6)$$

5. Removal Cr(VI) from Simulated Wastewater

Inorganic anions, like Cl^-, NO_3^-, PO_4^{3-}, SO_4^{2-}, and CO_3^{2-}, are widely distributed in wastewater, which usually affects the removal performance of contaminants [40]. The effect of co-existing ions on the Cr(VI) removal was checked in detail. As shown in Fig. 5(a), the added Cl^- and NO_3^- slightly decreases the removal efficiency of Cr(VI), which can be attributed to their weak coordination ability, producing nonsignificant impact on the SCG surface [41]. By contrast, SO_4^{2-} is more easily adsorbed on SCG surface, preventing the Cr(VI) removal. The inhibitory effect of PO_4^{3-} and CO_3^{2-} on Cr(VI) removal is the most significant. Compared with Cl^-, NO_3^- and SO_4^{2-}, the strong coordination ability of PO_4^{3-} causes intense competition for the same active sites with Cr(VI), resulting in the significantly retard the removal of Cr(VI) on SCG surface [42]. It is noted that CO_3^{2-} could react with the -COOH group containing compound by consuming H^+, leading to the inactivation of SCG sites, and thus strongly inhibiting the Cr(VI) removal.

Humic acid (HA), a macromolecular organic matter widely found in nature, profoundly affects the Cr(VI) removal performance [43]. As shown in Fig. 5(b), the Cr(VI) removal efficiency of SCG in the presence of different concentrations of HA (0-80 mg/L) was also evaluated. The Cr(VI) removal rate slightly decreases by 4% with the increase in HA concentration from 5 to 20 mg/L, while the removal efficiency decreases by 10% from 40 to 80 mg/L. Probably, the HA with a mass of carboxyl groups could competitively coordinate the Cr(VI) anions in the aqueous [44,45], and thus inhibit the Cr(VI) removal by SCG. In addition, a reusability test of SCG on the removal of Cr(VI) was conducted and the result is shown in Fig. 5(c). The Cr(VI) was completely removed in 30 min for the first four consecutive times, indicating the good reusability of SCG. At the fifth reusability, the removal efficiency of Cr(VI) decreased approximately 10%, which was probably attributed to the partial destruction of O- and N-containing groups on SCG during the regeneration and reutilization process.

6. Column Experiment

The Cr(VI) contaminant easily migrated into groundwater, where the treatment was required the permeable reactive barriers (PRB) technology [46,47]. As was reported, the zero-valent iron-bearing permeable reactive barrier (PRB) technology was developed owing to its cost-effectiveness and reduction performance. However, zero-valent iron suffered the faster passivation and greater porosity loss, which is not beneficial for the long-term performance of PRBs [48]. By contrast, the Cr(VI) removal performance by using SCG in this study was more preeminent than zero-valent iron. Besides, the fluffy structure of SCG benefited the Cr(VI)-containing groundwater flow across the column. Both reasons indicated that SCG would be an alternative active material in PRB to treat the Cr(VI)-containing groundwater. Therefore, a column experiment was used to simulate the PRB technology by using SCG as the reactive medium. The SCG packed column reactor system was designed to check the long-term performance of SCG (Fig. S6). As shown in Fig. 5(d), in the initial stage, Cr(VI) is almost never detected in the effluent, suggesting the perfect adsorption and reduction performance of SCG. With increased the effluent solution to 2,600 mL, the effluent concentrations of Cr(VI) increase and quickly reach the saturation point. According to the mass of SCG packed in column and the initial concentration of Cr(VI), the accumulated amount of Cr(VI) adsorbed onto SCG reaches 5.2 mg/g, which is larger than that of zero-valent iron [49,50]. The excellent Cr(VI) removal performance suggests that the SCG might be a promising alternative to remove the Cr(VI)-containing groundwater in the permeable reactive barrier [51].

7. Enhanced Cr(VI) Removal Mechanism of SCG

Based on the above results, the interface adsorption and reduction mechanism of Cr(VI) on SCG were clarified (Scheme 1). SCG contained lignocelluloses and organic compounds such as caffeine and phenolic compounds, endowing it with abundant surface O and N-containing functional groups. ATR-FTIR verified that a hydrogen bond was formed between the O and N-containing functional groups on SCG and $HCrO_4^-$ anions. In the pre-adsorption of Cr(VI) process, $HCrO_4^-$ ions were directly adsorbed on the surface of SCG via the formed hydrogen bond of SCG-COOH/

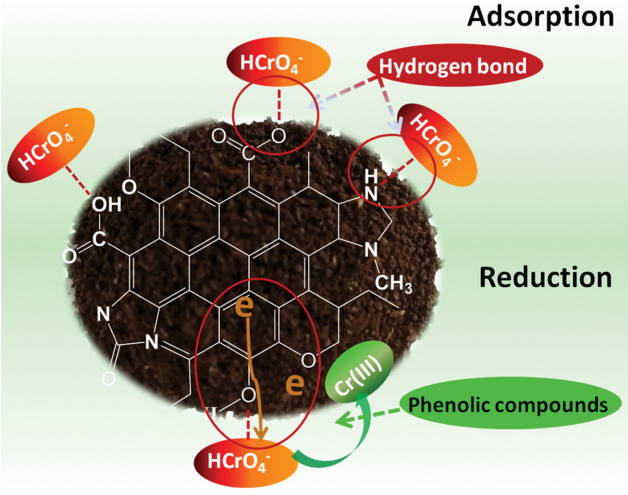

Scheme 1. Schematic for the adsorption and reduction pathway of Cr(VI) on SCG.

-OH···$HCrO_4^-$ and SCG-NH···$HCrO_4^-$. The electrons from reductive phenolics which contained abundant -OH were quickly transferred to $HCrO_4^-$ as soon as the $HCrO_4^-$ adsorbed on SCG, while the -COOH and -NH-containing compounds were mainly responsible for the Cr(VI) adsorption. This study confirms the important role of hydrogen bond formed between the O and N-containing functional groups on SCG and $HCrO_4^-$ anions. The reusability of SCG and column experiment proves the promising application of SCG for the removal of Cr(VI)-contaminated wastewater.

CONCLUSIONS

The mobility and biotoxicity of Cr(VI) cause great harm to human health and aquatic life. In addition to the widely reported zero-valent iron, biochar, and other nanocomposites, spent coffee ground (SCG) is a desirable alternative to remove Cr(VI) with a maximum uptake of 36.2 mg/g. In the study, we first systematically explored the interfacial adsorption and reduction process of Cr(VI) ions on SCG with the eliminated carboxyl and hydroxyl groups experiments and ATR-FTIR spectroscopy. The result revealed that the $HCrO_4^-$ was pre-adsorbed on SCG surface driven by the formed hydrogen bond of SCG-COOH/-OH···$HCrO_4^-$ and SCG-NH···$HCrO_4^-$. Then the partial $HCrO_4^-$ was quickly reduced to Cr(III) by the devoted electron from the phenolic compound present on SCG, followed by *in-situ* Cr(III) immobilization. Besides, the investigation of the coexisting ions and humic acid on the Cr(VI) removal, and column experiments further indicated SCG would be a new ideal substitute for the Cr(VI)-contaminated wastewater treatment. This study uncovered the adsorption and reduction mechanism of Cr(VI) removal on SCG and also provided some clues for the efficient treatment of Cr(VI).

ACKNOWLEDGEMENTS

This work was supported by the Characteristic Innovation Projects Guangdong Provincial Department of Education (Natural Science Category, 2018KTSCX208 and 2021KQNCX084), Guangdong Basic and Applied Basic Research Foundation (2021A1515010185), the Science and Technology Project of Guangdong Province (Shaoguan Science and Technology Bureau [2020] No. 44), the Projects of Science and Technology of Shaoguan City (2018sn057 and 200811094530800), the Shaoguan University Research Project (SZ2020KJ04 and SY2020KJ04), the Student Science and Technology Innovation Cultivating Program of Guangdong Province (pdjh2021b0457), and the Student Innovation and Entrepreneurship Training Program of China (S202010576029).

SUPPORTING INFORMATION

Additional information as noted in the text. This information is available via the Internet at http://www.springer.com/chemistry/journal/11814.

REFERENCES

1. E. Kaprara, P. Seridou, V. Tsiamili, M. Mitrakas, G. Vourlias, I. Tsiaoussis, G. Kaimakamis, E. Pavlidou, N. Andritsos and K. Simeonidis, *J. Hazard. Mater.*, **262**, 606 (2013).
2. T. Liu, L. Zhao, D. Sun and X. Tan, *J. Hazard. Mater.*, **184**, 724 (2010).
3. Y. J. Lee, C. G. Lee, J. K. Kang, S. J. Park and P. J. J. Alvarez, *Environ. Sci. Water Res. Technol.*, **7**, 222 (2021).
4. C. G. Lee, J. A. Park, J. W. Choi, S. O. Ko and S. H. Lee, *Water Air Soil Pollut.*, **227**, 287 (2016).
5. J. Du, J. Bao, C. Lu and D. Werner, *Water Res.*, **102**, 73 (2016).
6. Y. Mu, Z. Ai, L. Zhang and F. Song, *ACS Appl. Mater. Inter.*, **7**, 1997 (2015).
7. D. Rodríguez-Padrón, M. J. Muñoz-Batista, H. Li, K. Shih, A. M. Balu, A. Pineda and R. Luque, *ACS Sustain. Chem. Eng.*, **7**, 17030 (2019).
8. A. S. Franca, L. S. Oliveira and M. E. Ferreira, *Desalination*, **249**, 267 (2009).
9. C. Monente, I. A. Ludwig, A. Irigoyen, M. P. De Pena and C. Cid, *J. Agric. Food Chem.*, **63**, 4327 (2015).
10. A. C. F. Alves, R. V. P. Antero, S. B. de Oliveira, S. A. Ojala and P. S. Scalize, *Environ. Sci. Pollut. Res. Int.*, **26**, 24850 (2019).
11. B. H. An, H. Jeong, J. H. Kim, S. Park, J. H. Jeong, M. J. Kim and M. Chang, *J. Agric. Food Chem.*, **67**, 8649 (2019).
12. H. Moustafa, C. Guizani, C. Dupont, V. Martin, M. Jeguirim and A. Dufresne, *ACS Sustain. Chem. Eng.*, **5**, 1906 (2017).
13. A. Panusa, A. Zuorro, R. Lavecchia, G. Marrosu and R. Petrucci, *J. Agric. Food Chem.*, **61**, 4162 (2013).
14. M. H. Park, J. Lee and J. Y. Kim, *Chemosphere*, **234**, 179 (2019).
15. S. K. Prabhakaran, K. Vijayaraghavan and R. Balasubramanian, *Ind. Eng. Chem. Res.*, **48**, 2113 (2009).
16. T. U. Han, J. Kim and K. Kim, *J. Ind. Eng. Chem.*, **100**, 310 (2021).
17. T. Tian, S. Freeman, M. Corey, J. B. German and D. Barile, *J. Agric. Food Chem.*, **65**, 2784 (2017).
18. D. R. Vardon, B. R. Moser, W. Zheng, K. Witkin, R. L. Evangelista, T. J. Strathmann, K. Rajagopalan and B. K. Sharma, *ACS Sustain. Chem. Eng.*, **1**, 1286 (2013).
19. N. Bardiya, Y. W. Hwang and J. H. Bae, *Anaerobe*, **10**, 7 (2004).
20. N. Zhao, C. Zhao, D. C. W. Tsang, K. Liu, L. Zhu, W. Zhang, J. Zhang, Y. Tang and R. Qiu, *J. Hazard. Mater.*, **404**, 124162 (2021).
21. T. Chen, Z. Zhou, S. Xu, H. Wang and W. Lu, *Bioresour. Technol.*, **190**, 388 (2015).
22. N. Zhao, Z. Yin, F. Liu, M. Zhang, Y. Lv, Z. Hao, G. Pan and J. Zhang, *Bioresour. Technol.*, **260**, 294 (2018).
23. Y. Hu, X. Peng, Z. Ai, F. Jia and L. Zhang, *Environ. Sci. Technol.*, **53**, 8333 (2019).
24. J. Li, X. Zhang, M. Liu, B. Pan, W. Zhang, Z. Shi and X. Guan, *Environ. Sci. Technol.*, **52**, 2988 (2018).
25. X. Lv, J. Xu, G. Jiang, J. Tang and X. Xu, *J. Colloid Interface Sci.*, **369**, 460 (2012).
26. C. Y. Cao, J. Qu, W. S. Yan, J. F. Zhu, Z. Y. Wu and W. G. Song, *Langmuir*, **28**, 4573 (2012).
27. Y. Hu, G. Zhan, X. Peng, X. Liu, Z. Ai, F. Jia, S. Cao, F. Quan, W. Shen and L. Zhang, *Chem. Eng. J.*, **389**, 124414 (2020).
28. J. Xu, Z. Cao, Y. Wang, Y. Zhang, X. Gao, M. B. Ahmed, J. Zhang, Y. Yang, J. L. Zhou and G. V. Lowry, *Chem. Eng. J.*, **359**, 713 (2019).
29. H. Xu, L. Xie, J. Li and M. Hakkarainen, *ACS Appl. Mater. Interf.*, **9**, 27972 (2017).

30. S. Zhu, S. H. Ho, X. Huang, D. Wang, F. Yang, L. Wang, C. Wang, X. Cao and F. Ma, *ACS Sustain. Chem. Eng.*, **5**, 9673 (2017).
31. S. Zhu, X. Huang, X. Yang, P. Peng, Z. Li and C. Jin, *Environ. Sci. Technol.*, **54**, 8123 (2020).
32. H. Zhu, X. Tan, L. Tan, C. Chen, N. S. Alharbi, T. Hayat, M. Fang and X. Wang, *ACS Appl. Nano Mater.*, **1**, 2689 (2018).
33. E. D. Flynn and J. G. Catalano, *Environ. Sci. Technol.*, **51**, 9792 (2017).
34. X. Huang, X. Hou, F. Song, J. Zhao and L. Zhang, *Environ. Sci. Technol.*, **50**, 1964 (2016).
35. T. Jozwiak, U. Filipkowska, J. Struk-Sokolowska, K. Bryszewski, K. Trzcinski, J. Kuzma and M. Slimkowska, *Sci. Rep.*, **11**, 9584 (2021).
36. G. Sharma, M. Naushad, A. H. Al-Muhtaseb, A. Kumar, M. R. Khan, S. Kalia, Shweta, M. Bala and A. Sharma, *Int. J. Biol. Macromol.*, **95**, 484 (2017).
37. X. Cao, J. Guo, J. Mao and Y. Lan, *J. Hazard. Mater.*, **192**, 1533 (2011).
38. Y. Li, B. Xing, X. Wang, K. Wang, L. Zhu and S. Wang, *Energ. Fuel*, **33**, 12459 (2019).
39. X. Wang, Y. Qin, L. Zhu and H. Tang, *Environ. Sci. Technol.*, **49**, 6855 (2015).
40. T. Almeelbi and A. Bezbaruah, *J. Nanoparticle Res.*, **14**, 197 (2012).
41. H. Wang, X. Liang, Y. Liu, T. Li and K. Y. A. Lin, *Resour. Conserv. Recycl.*, **168**, 105284 (2021).
42. X. Lv, Y. Hu, J. Tang, T. Sheng, G. Jiang and X. Xu, *Chem. Eng. J.*, **218**, 55 (2013).
43. H. Dong and I. M. Lo, *Water Res.*, **47**, 419 (2013).
44. T. Liu, P. Rao, M. S. Mak, P. Wang and I. M. Lo, *Water Res.*, **43**, 2540 (2009).
45. Q. Wang, N. Cissoko, M. Zhou and X. Xu, *Phys. Chem. Earth*, **36**, 442 (2011).
46. P. Agrawal and A. K. Bajpai, *J. Disper. Sci. Technol.*, **32**, 1353 (2011).
47. F. He, M. Zhang, T. Qian and D. Zhao, *J. Colloid Interface Sci.*, **334**, 96 (2009).
48. Y. Fang, X. Wu, M. Dai, A. Lopez-Valdivieso, S. Raza, I. Ali, C. Peng, J. Li and I. Naz, *J. Clean. Prod.*, **312**, 127678 (2021).
49. J. Zhong, W. Yin, Y. Li, P. Li, J. Wu, G. Jiang, J. Gu and H. Liang, *Water Res.*, **122**, 536 (2017).
50. J. Dries, L. Bastiaens, D. Springael, S. Kuypers, S. N. Agathos and L. Diels, *Water Res.*, **39**, 3531 (2005).
51. Z. Yang, C. Shan, W. Zhang, Z. Jiang, X. Guan and B. Pan, *Water Res.*, **106**, 461 (2016).

Supporting Information

Efficient removal of Cr(VI) by spent coffee grounds: Molecular adsorption and reduction mechanism

Yue Hu, Meiting Zhi, Shilin Chen, Wenguan Lu, Yinlong Lai, and Xiaobing Wang†

School of Chemistry and Civil Engineering, Shaoguan University, Shaoguan, 512023, P. R. China
(*Received 14 October 2021 • Revised 28 November 2021 • Accepted 16 December 2021*)

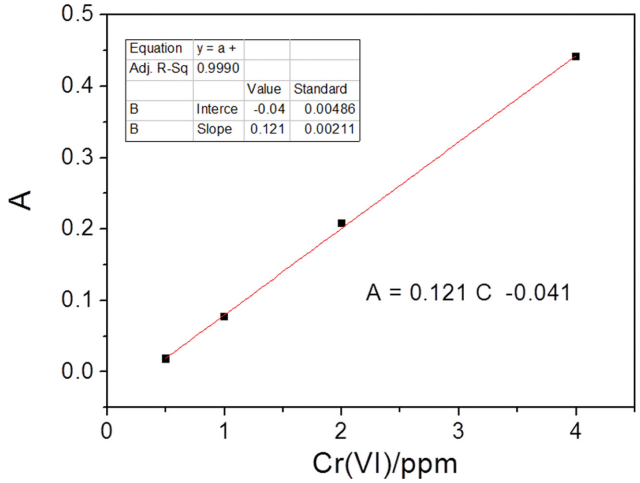

Fig. S1. Absorbance of different Cr(VI) concentration checked by the 1,5-diphenylcarbazide colorimetric method.

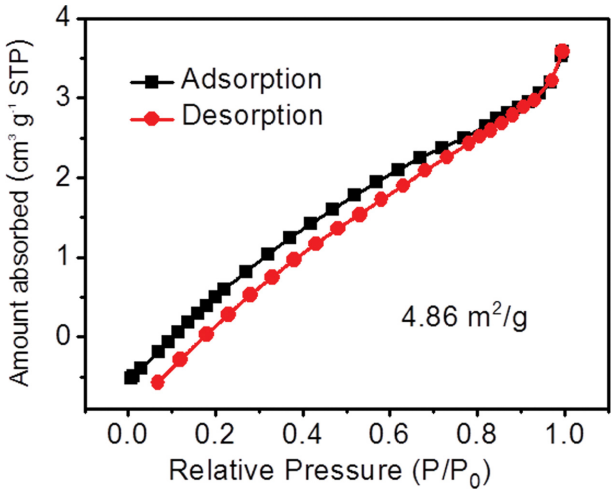

Fig. S2. Nitrogen adsorption-desorption isotherms of SCG.

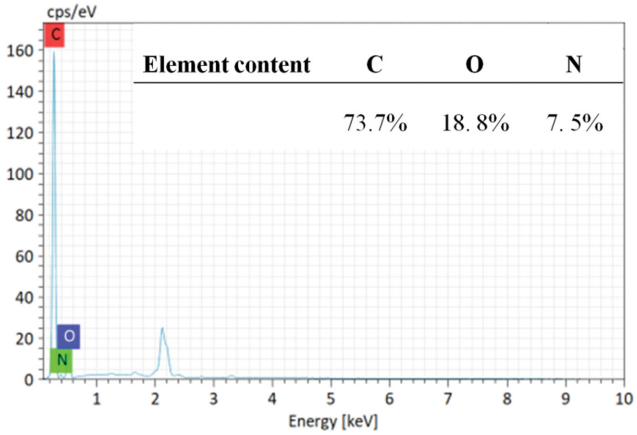

Fig. S3. Energy-dispersive X-ray spectroscopy (EDS) of SCG.

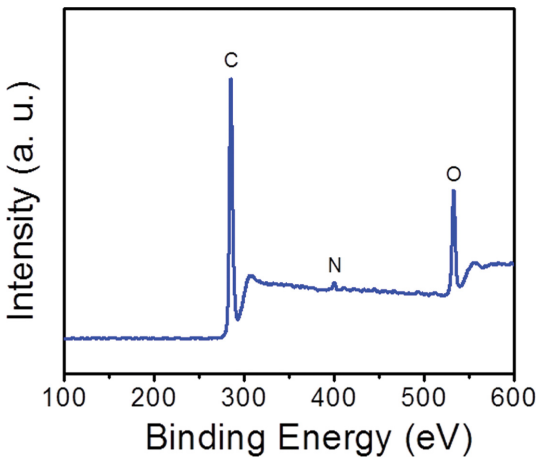

Fig. S4. XPS spectroscopy of SCG.

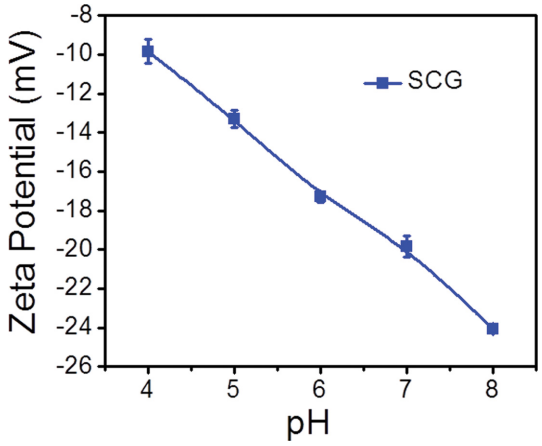

Fig. S5. Zeta potential of SCG at initial pH 4-8.

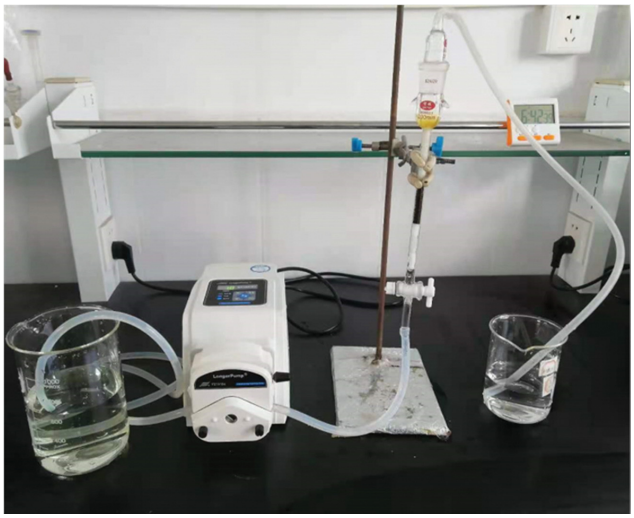

Fig. S6. SCG-packed column reactor system.

Table S1. Remove quantity of Cr(VI) by SCG

Cr(VI)/(mg/L)	2	5	10	20	50	100
Remove quantity/(mg/L)	2	5	10	18	32.5	30.0

Table S2. Comparison of the maximum Cr(VI) removal by SCG, biochar, zero-valent iron-based adsorbent and iron oxides. (SSA: specific surface area)

Samples	Initial pH	SSA (m^2/g)	q_m (mg/g)	q_m (mg/m^2)	Reference
SCG	7.0	4.86	36.2	7.4	This work
Oak wood biochar	2.0	/	3.03	/	[1]
Corn straw biochars	7.0	417.83	26.2	0.062	[2]
ZVI	6.2	0.75	0.87	1.16	[3]
S-ZVI$_{Na2S}$	6.0		30.8		[4]
nZVI-Fe_3O_4	8.0	40	29.43	0.14	[5]
α-Fe_2O_3	3.0	120	30	0.23	[6]

REFERENCES

1. T. Chen, Z. Zhou, S. Xu, H. Wang and W. Lu, *Bioresour. Technol.*, **190**, 388 (2015).
2. N. Zhao, Z. Yin, F. Liu, M. Zhang, Y. Lv, Z. Hao, G. Pan and J. Zhang, *Bioresour. Technol.*, **260**, 294 (2018).
3. Y. Hu, X. Peng, Z. Ai, F. Jia and L. Zhang, *Environ. Sci. Technol.*, **53**, 8333 (2019).
4. J. Li, X. Zhang, M. Liu, B. Pan, W. Zhang, Z. Shi and X. Guan, *Environ. Sci. Technol.*, **52**, 2988 (2018).
5. X. Lv, J. Xu, G. Jiang, J. Tang and X. Xu, *J. Colloid Interface Sci.*, **369**, 460 (2012).
6. C. Y. Cao, J. Qu, W. S. Yan, J. F. Zhu, Z. Y. Wu and W. G. Song, *Langmuir*, **28**, 4573 (2012).